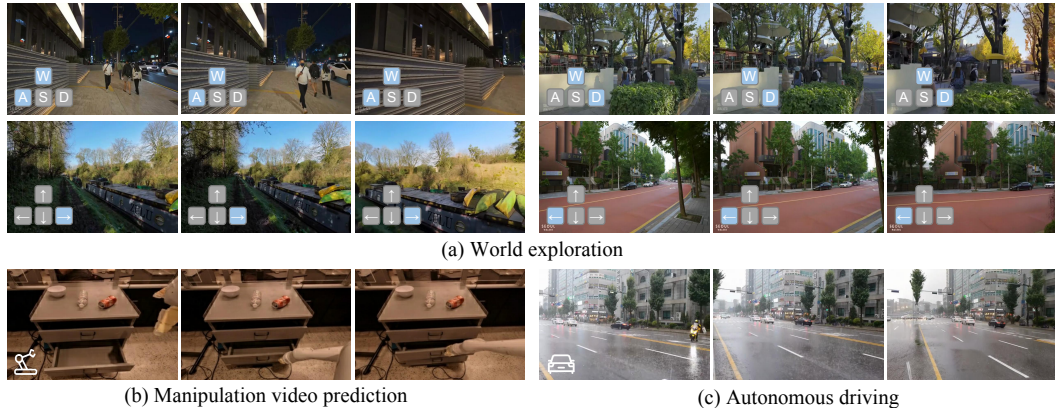


000 001 ASTRA GENERAL INTERACTIVE WORLD MODEL 002 WITH AUTOREGRESSIVE DENOISING 003 004

005 **Anonymous authors**
006 Paper under double-blind review
007



021 Figure 1: Our *Astra* enables interactive and versatile world modeling across exploration, robotics,
022 and autonomous driving. With our enhanced design spanning framework architecture to training and
023 inference, it delivers precise responsiveness to user instructions and strong long-term consistency,
024 achieving coherent high-fidelity videos that faithfully follow instructions.

025 ABSTRACT 026

027 Recent advances in diffusion transformers have empowered video generation
028 models to generate high-quality video clips from texts or images. However, world
029 models with the ability to predict long-horizon futures from past observations
030 and actions remain underexplored, especially for general-purpose scenarios and
031 various forms of actions. To bridge this gap, we introduce *Astra*, an interactive
032 general world model that generates real-world futures for diverse scenarios (e.g.,
033 autonomous driving, robot grasping) with precise action interactions (e.g., camera
034 motion, robot action). We propose an autoregressive denoising architecture and
035 use temporal causal attention to aggregate past observations and support stream-
036 ing outputs. We use a noise-augmented history memory to avoid over-reliance
037 on past frames to balance responsiveness with temporal coherence. For precise
038 action control, we introduce an action-aware adapter that directly injects action
039 signals into the denoising process. We further develop a mixture of action ex-
040 perts that dynamically route heterogeneous action modalities, enhancing versatil-
041 ity across diverse real-world tasks such as exploration, manipulation, and camera
042 control. *Astra* achieves interactive, consistent, and general long-term video pre-
043 diction and supports various forms of interactions. Experiments across multiple
044 datasets demonstrate the improvements of *Astra* in fidelity, long-range prediction,
045 and action alignment over existing state-of-the-art world models.

046 1 INTRODUCTION 047

048 Building generative world models is an emerging field where the ability to synthesize realistic and
049 coherent video trajectories serves as a proxy for understanding and simulating the underlying
050 dynamics of the world. With the rapid advances in visual generation (Rombach et al., 2022; Blattmann
051 et al., 2023; Yang et al., 2025; Brooks et al., 2024; Wan et al., 2025), numerous video genera-
052 tion models have emerged and can perceive contextual cues and synthesize high-fidelity videos of
053 open-world scenarios. These advances serve as the foundation for broader world simulation tasks,
including game engines, autonomous driving, and spatial intelligence.

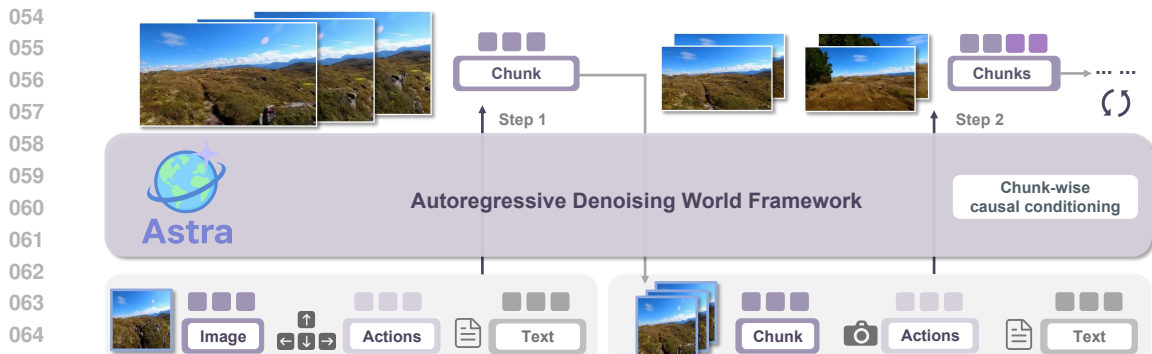


Figure 2: **Overview of the proposed Astra.** Our autoregressive denoising world model generates future video chunk by chunk from an initial image, actions, and optional prompts. Chunk-wise causal conditioning enforces temporal coherence and faithful action response.

Standard text-to-video (T2V) or image-to-video (I2V) models typically produce only short, self-contained video clips conditioned on prompts or reference images. They lack the ability to generate coherent long-horizon rollouts that respond adaptively to external stimuli such as agent movements, viewpoint changes, or control signals. Without this responsiveness, these models fall short of simulating the interactive and causal dynamics of the real world. Furthermore, existing video generators are constrained by the finite temporal window of diffusion models, which prevents them from producing extended video sequences. Although recent works (Mao et al., 2025; He et al., 2025; Song et al., 2025; Teng et al., 2025) have explored video continuation techniques or hybrid frameworks that combine autoregression with diffusion, they often struggle to strike a balance between maintaining consistency with historical frames and remaining responsive to new inputs. In addition, the autoregressive generation process introduces error accumulation, leading to degraded quality and coherence in long-term predictions. As a result, despite impressive progress in generative fidelity, existing approaches remain largely passive—capable of rendering visually compelling content yet lacking the interactivity, adaptability, and robustness required for true world simulation.

To address these challenges, we present Astra, a simple yet powerful framework for building highly interactive world models. At its core, our method adopts an autoregressive denoising paradigm, where we augment a pre-trained video diffusion backbone with an action-aware adapter, as shown in Figure 2. This design preserves the high generative quality of diffusion models while enabling precise conditioning on agent actions, thereby allowing the model to produce coherent futures that respond instantly to user inputs. A central difficulty in world modeling is balancing long-term temporal consistency with action responsiveness. To mitigate this, we propose a noise-as-mask strategy that softly corrupts historical frames during training. This reduces the dominance of visual context, forcing the model to integrate both history and action cues when predicting the next video chunk. Moreover, real-world interactive environments involve heterogeneous action modalities—from camera controls and body pose to robot manipulations. To enhance versatility across such settings, we design a Mixture of Action Experts (MoAE), where modality-specific experts specialize in different action types under a learnable routing mechanism. This enables our model to unify diverse interaction signals within a single framework, making it broadly applicable across scenarios spanning embodied robotics, immersive video simulation, and long-horizon world exploration.

We conduct extensive experiments on diverse open-source benchmarks, including Sekai (Li et al., 2025a), SpatialVID (Wang et al., 2025), RT-1 (Brohan et al., 2022), nuScenes (Caesar et al., 2020) and Multi-Cam Video (Bai et al., 2025). As illustrated in Figure 1, Astra achieves state-of-the-art performance in action-driven video prediction, generating sequences that are highly interactive while maintaining visual coherence and dynamic consistency. Furthermore, our framework also demonstrates strong generalization across tasks and environments, underscoring its potential as a foundation for next-generation visual world models.

2 RELATED WORK

Video generation models. In recent years, denoising diffusion models (Ho et al., 2020; Song et al., 2020) have become the dominant paradigm in generative modeling, celebrated for their high fidelity

108 and controllability. Following their success in text-to-image (T2I) synthesis (Rombach et al., 2022;
 109 Dhariwal & Nichol, 2021), early video generation methods (Blattmann et al., 2023; Ho et al., 2022)
 110 extended diffusion models to the temporal domain, typically by inflating image-based UNets (Ron-
 111 neberger et al., 2015) with additional temporal layers. More recently, Sora (Brooks et al., 2024)
 112 and following studies (Zheng et al., 2024; Yang et al., 2025; Ma et al., 2024) pioneer high-quality,
 113 high-resolution text-to-video (T2V) diffusion models. These models commonly use the diffusion
 114 transformer (DiT) architecture (Peebles & Xie, 2023) to capture complex spatial and temporal co-
 115herence. More recent models, including (Song et al., 2025) and (Zhang & Agrawala, 2025), further
 116 improve long-horizon consistency. Beyond pure diffusion, hybrid frameworks have been proposed
 117 to reconcile long-range prediction with high-quality synthesis. By combining autoregression for
 118 temporal modeling and diffusion for local realism, approaches such as StreamingT2V (Henschel
 119 et al., 2025) and MAGI (Teng et al., 2025) achieve extended video rollouts. However, these meth-
 120 ods still struggle with error accumulation across long sequences and offer limited responsiveness to
 121 external actions, leaving a gap between video generation and true interactive world simulation.

122 **Visual world models.** Beyond video generation, visual world models aim to capture the causal
 123 dynamics of the environment, enabling agents to simulate future trajectories and interact with the
 124 world. Unlike text-to-video or image-to-video models that generate short clips conditioned on static
 125 inputs, visual world models explicitly incorporate history and actions, making them essential for
 126 tasks such as planning, control, and embodied intelligence. Several recent works demonstrate this
 127 trend. (Wu et al., 2024) extends autoregressive video transformers to integrate actions and rewards,
 128 allowing agents to predict how future observations evolve in interactive environments. (Wang et al.,
 129 2024) formulates world modeling as masked-token prediction in discrete latent space, supporting
 130 multimodal conditioning and open-ended environment simulation. (Huang et al., 2025; He et al.,
 131 2025) adapts pretrained video diffusion models into an autoregressive framework with causal action
 132 guidance, making them capable of controllable video prediction. In navigation contexts, (Bar et al.,
 133 2025) employs conditional diffusion-transformers to generate plausible future agent observations,
 134 facilitating planning in unfamiliar scenes. Meanwhile, (Cen et al., 2025) introduces a joint vision-
 135 language-action (VLA) framework that learns to model both world states and agent behaviors in an
 136 autoregressive manner. At larger scales, frameworks such as (Bruce et al., 2024; Agarwal et al.,
 137 2025; Liu et al., 2024) demonstrate that scaling up transformer architectures and extending context
 138 windows significantly improve rollout fidelity and generalization across domains. Recently, (Mao
 139 et al., 2025) uses a Masked Video Diffusion Transformer (MVDT) to selectively mask input features
 140 to improve video generation quality. In contrast, Astra employs a noise-as-mask strategy to partially
 141 degrade historical visual context, encouraging the model to integrate action signals more effectively
 142 and respond accurately to user commands. These methods highlight the growing potential of world
 143 models for simulating interactive, versatile, and controllable environments. Nonetheless, they of-
 144 ten suffer from issues such as error accumulation, temporal inconsistency in long-horizon rollouts,
 145 and limited responsiveness to arbitrary actions. Addressing these challenges remains crucial for
 146 developing reliable and scalable visual world models.

3 PROPOSED APPROACH

147 In this section, we present Astra, an autoregressive denoising framework that achieves real-world
 148 video prediction and enjoys high interactivity, versatility, and consistency. Our key idea is to harness
 149 the visual generation power within a pre-trained text-to-video diffusion model and incorporate the
 150 chunk-wise autoregressive prediction by using previously generated clips as conditions. We will
 151 start by reviewing the background of autoregressive denoising models, and then describe our designs
 152 of Astra, including an action-aware adapter for precise conditioning and a noise-augmented history
 153 memory for long-term consistency, and a mixture of action experts (MoAE) for unifying diverse
 154 action inputs. The overall framework of our Astra is illustrated in Figure 3.

3.1 PRELIMINARY: AUTOREGRESSIVE DENOISING MODEL

155 We adopt an autoregressive denoising framework, which integrates the long-horizon modeling of
 156 autoregression with the high-fidelity synthesis of diffusion. Given a video sequence discretized into

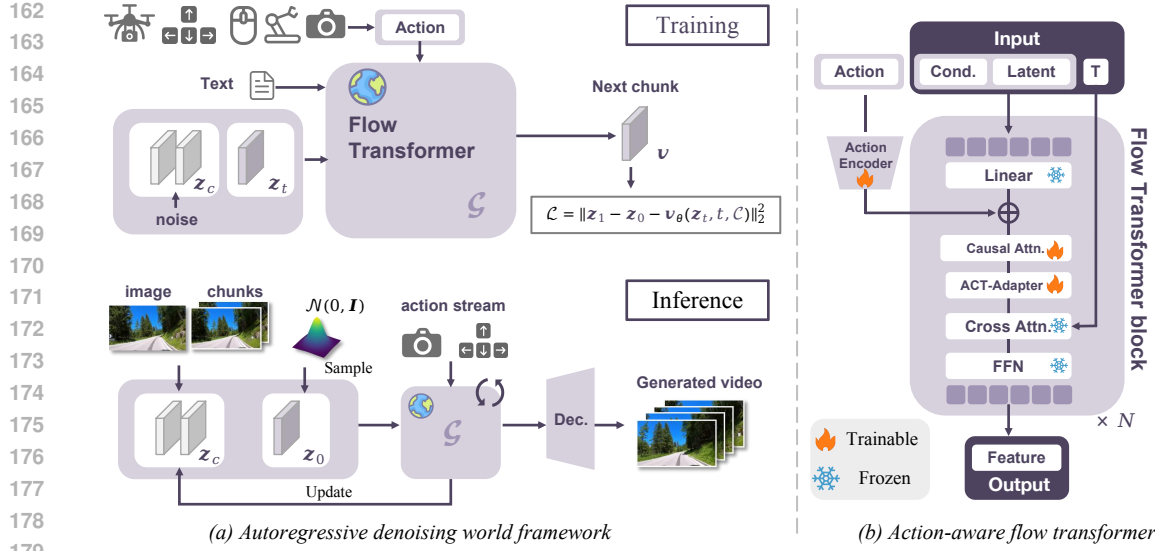


Figure 3: **The overall framework of Astra.** The Action-Aware Flow Transformer (AFT) injects action signals into the latent space via an ACT-Adapter (right), which aligns action features through an encoder and adds them to each transformer block. During training (left top), the model learns next-chunk prediction with flow matching. During inference (left bottom), it autoregressively generates video chunks conditioned on history and action streams, producing interactive videos.

chunks $z^{1:N}$, the generation objective is:

$$p(z^{1:N}) = \prod_{i=1}^N p(z^i | z^{<i}). \quad (1)$$

For each step, the next chunk z_{t+1} is predicted through a denoising process, trained using flow matching. Specifically, we first sample a noisy interpolation of the target chunk:

$$z_t^i = (1 - t)z_0^i + t\epsilon, \quad \epsilon \sim \mathcal{N}(0, I), \quad t \in [0, 1], \quad (2)$$

and train the flow model v_θ to estimate the clean direction:

$$\mathcal{L}(\theta) = \mathbb{E}_{i, t, \epsilon} \left[\|v_\theta(z_t^i, t | z^{<i}) - v^*(z_t^i, t | z^{<i})\|_2^2 \right], \quad (3)$$

where v^* is the ground-truth velocity. In inference, autoregressive generation proceeds by denoising from noise to obtain z^{i+1} , which is then appended to history for predicting future chunks. This iterative AR-denoising loop enables long-range, consistent, and high-quality video prediction.

3.2 INTERACTIVE WORLD MODELING VIA AUTOREGRESSIVE DENOISING

Modern video generation models (Brooks et al., 2024; Wan et al., 2025) have demonstrated remarkable progress in simulating realistic visual dynamics. These models benefit from large-scale pretraining, which enables them to implicitly acquire partial knowledge of 3D spatial perception, temporal dependencies, and even simple physical patterns such as motion and force. However, despite their impressive fidelity, these models still fall short in constructing real-world scenes that can be preserved, interacted and explored. This raises a key question: *Are T2V models really world models?* In our view, the defining property of a world model is interactivity—the ability to adapt generation dynamically in response to arbitrary action inputs at arbitrary moments. While diffusion-based models can be conditioned on global prompts or scene attributes, such conditioning mechanisms do not enable fine-grained, online interaction. To address this limitation, we turn to the autoregressive framework, which naturally supports stepwise prediction conditioned on both past observations and current actions. Unlike diffusion models that generate video in a single pass, autoregression allows for instantaneous responses to action inputs, enabling controllable and adaptive rollouts. By

216 integrating this property with the generative power of denoising models, we design an autoregressive
 217 denoising framework that achieves both high-quality synthesis and interactive controllability.
 218 Although prior works have explored combining autoregression and denoising, reconstructing this
 219 hybrid paradigm for world modeling remains non-trivial. Beyond simply chaining autoregression
 220 and denoising, we must carefully define the observation–action interface and design mechanisms to
 221 balance the trade-off between long-term consistency and immediate responsiveness

222 Given the previous video chunks $z^{1:i-1}$, we aim to model the conditional distribution of the next
 223 chunk $p(z^i|z^{1:i-1})$. In principle, this prediction can be realized by a variety of generative models.
 224 To ensure high visual fidelity, we choose to leverage a pre-trained video flow matching model v_θ as
 225 the predictor, leveraging its strong video synthesis capability. However, integrating such a model into
 226 an interactive world framework introduces two central challenges: (1) How to represent actions and
 227 quantify their impact on future visual dynamics; (2) How to effectively incorporate action signals
 228 into a pre-trained diffusion backbone while preserving its generative quality.

229 Since our goal is to enable instantaneous responses to action inputs a^i (e.g., an instruction such
 230 as “turn right”), the effect of an action should manifest as a direct transformation on the predicted
 231 video chunk. Inspired by the formulation of optical flow, we interpret this transformation as a shift
 232 in video features, which, in diffusion models, correspond to latent representations within the de-
 233 noiser. Accordingly, we treat the action as an additional conditioning signal for the diffusion model,
 234 applied directly to its latent feature space. This requirement poses a challenge for existing video
 235 diffusion architectures, which are typically composed of stacked Transformer blocks (DiT) and rely
 236 on cross-attention layers to align video latents with textual embeddings. Such mechanisms are not
 237 naturally suited for modeling fine-grained action-induced shifts. To overcome this, we introduce the
 238 action-aware flow transformer adapter (ACT-Adapter) that augments a pre-trained video DiT into an
 239 autoregressive denoising model capable of integrating action signals as latent-space transformations,
 240 preserving the generative power of the backbone while modeling the action’s influence.

241 As shown in Figure 3, we introduce an action encoder to project actions into a feature space aligned
 242 with the video latents. The resulting action features are injected into the denoising model through
 243 element-wise addition at every block, ensuring that action signals directly modulate the latent rep-
 244 resentation. To maximize reuse of pre-trained knowledge, we freeze all parameters of the flow
 245 transformer except for the self-attention layers. In addition, we insert a lightweight adapter mod-
 246 ule—a single linear layer initialized as the identity matrix—after each self-attention block. This
 247 enables the model to gradually learn action-aware transformations while maintaining the stability
 248 of the pre-trained backbone. For the history condition $z_c = z^{1:i-1}$, we adopt the frame-dimension
 249 conditioning strategy that concatenates the previous chunks with the predicted chunk along the tem-
 250 poral dimension before being processed by the flow transformer. Together with the action a^i and
 251 prompt c , the full condition set for the denoising model v_θ is $\mathcal{C} = \{z^{1:i-1}, a^{1:i}, c\}$.

252 To enhance the effect of actions, we propose an action-free guidance mechanism (AFG), inspired
 253 by class-free guidance (CFG). During training, action conditions are randomly dropped, forcing the
 254 model to predict without action inputs. At inference, we compute a guided velocity field:

$$v_{\text{guided}} = v_\theta(z_t, t, \emptyset) + s \cdot (v_\theta(z_t, t, a) - v_\theta(z_t, t, \emptyset)), \quad (4)$$

255 where s is the guidance scale, z_t is the combined latent and \emptyset denotes the null-action condition. This
 256 technique sharpens the action effect, yielding more precise responses to user inputs.

257 3.3 HISTORY CONDITION WITH NOISY MEMORY

258 After addressing the challenge of action control, we turn to another open problem: balancing the
 259 long-term temporal consistency with responsiveness to actions. Prior works have shown that gen-
 260 erating coherent long videos requires conditioning on an extended history. However, we observe
 261 a trade-off: increasing the length of history improves temporal consistency but weakens action re-
 262 sponsiveness. We refer to this phenomenon as *visual inertia*—the tendency of the model to rely
 263 heavily on past visual information while overlooking user actions. This arises because real-world
 264 datasets contain predominantly smooth motions, leading the model to prioritize continuity over
 265 abrupt, action-driven changes. To mitigate this inherent contradiction, we avoid naively shortening
 266 the conditioning horizon and instead seek a more elegant solution. Considering the asymmetry
 267 between dense visual inputs and sparse action signals, we propose to reduce the dominance of vi-
 268 sual conditioning by introducing controlled corruption. Unlike (Mao et al., 2025), which randomly

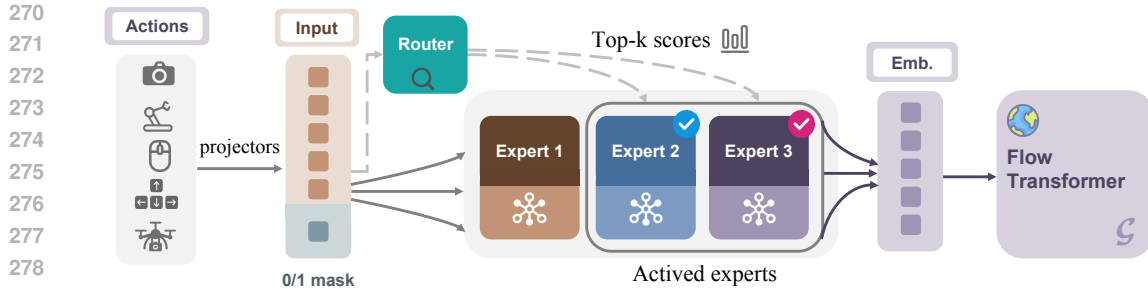


Figure 4: **Mixture of Action Experts (MoAE)**. Action signals from diverse modalities are projected into a shared space, augmented with a history mask, and routed to modality-specialized experts. A dynamic router selects top- k experts, whose outputs are aggregated into unified embeddings and fed into the Flow Transformer, enabling versatile and precise action-conditioned generation.

masks visual tokens, we adopt a noise-as-mask strategy: injecting random noise into the conditioning video to degrade and blur its information content (Figure 3). This design offers two advantages. First, it requires no architectural modifications or additional learnable parameters in the denoising model. Second, by corrupting the visual context, it prevents the model from directly copying clean frames and forces it to integrate action cues into generation. The corruption noise is independent of diffusion noise, so inference can use clean historical frames. Through this training strategy, the model learns to balance reliance on action and history, thereby overcoming visual inertia. To further extend the effective history horizon, we adopt the compression approach of (Zhang & Agrawala, 2025), which retains the first frame while compressing the intermediate history into compact visual tokens, preserving long-range temporal information without overwhelming the action signal.

3.4 MIXURE OF ACTION EXPERTS FOR DIVERSE SCENARIOS

Interactive world modeling often involves multi-modal inputs, including camera observations, body pose, and discrete action commands. These heterogeneous signals differ in structure and scale, making it challenging for a single model to capture their characteristics. To address this, we propose the Mixture of Action Experts (MoAE), a modular framework that routes different modalities to specialized experts, producing a unified action representation for the denoising model.

As shown in Figure 4, each action modality—continuous camera pose a_{cam} , robot pose a_{rob} , and discrete keyboard/mouse commands a_{cmd} —is first mapped into a shared action space via a modality-specific projector \mathcal{R}_m as $\tilde{a}^i = \mathcal{R}_m(a_m^i)$, where $m \in \{cam, rob, cmd\}$ denotes the specific modality and i is the sequence index. A router network then computes gating scores $\mathbf{g}^i = \text{Router}(\tilde{a}^i)$ to select the top- K relevant experts. Each chosen expert E_k , implemented as independent MLPs, transforms the aligned features into task-relevant representations. The expert outputs are then aggregated according to the router’s gating scores to produce the final action embedding $\mathbf{e}^i = \sum_{k=1}^K g_k^i E_k(\tilde{a}^i)$. The embedding sequence $\mathbf{e}^{1:i}$ is then fed into the flow transformer. To account for both historical and current actions, we augment the action space of \tilde{a}^i with an additional binary indicator specifying whether the input corresponds to a past or current action.

Combining MoAE with history-conditioned latent inputs allows the model to generate video chunks that are temporally coherent and responsive across modalities. This design improves modality specialization, scalability to new signals, efficiency by activating only relevant experts, and overall versatility, enabling high-fidelity predictions in complex interactive scenarios.

4 EXPERIMENT

4.1 EXPERIMENT SETUPS

Datasets. To train our model, we leverage a diverse set of datasets covering autonomous driving, egocentric exploration, multi-camera rendering, and robot control. Specifically, we use nuScenes (Caesar et al., 2020) for vehicle pose prediction, Sekai (Li et al., 2025a) and SpatialVID (Wang et al., 2025) for large-scale in-the-wild videos with rich camera annotations, Multi-

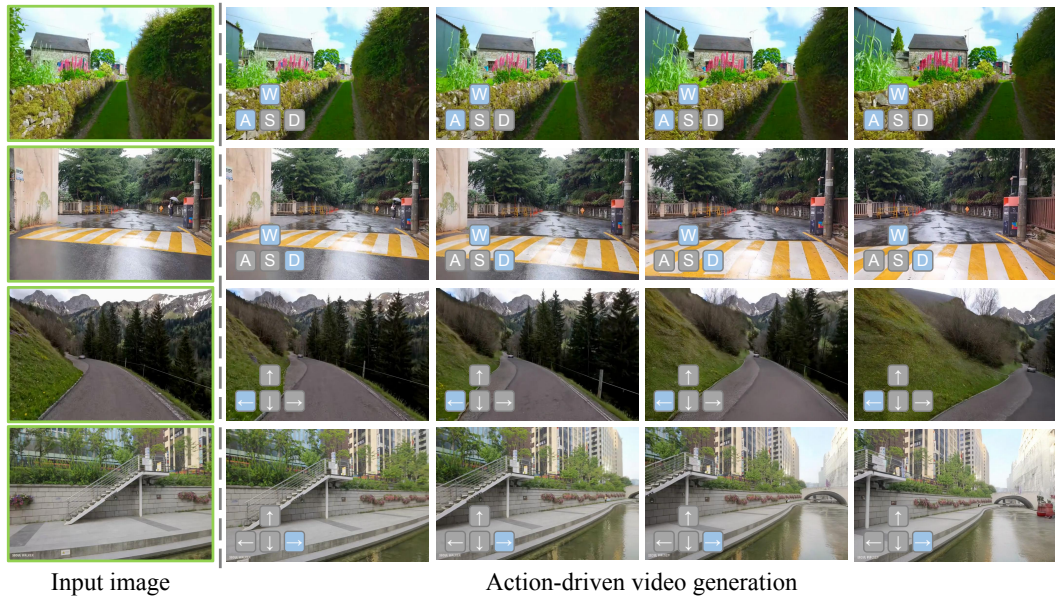


Figure 5: **Qualitative results on action-driven real-world exploration.** Starting from a single initial frame, our model generates long-term exploration videos with high visual fidelity, smooth and coherent dynamics, and precise responsiveness to action inputs.

Cam Video (Bai et al., 2025) for synthetic multi-view sequences, and RT-1 (Brohan et al., 2022) (via Open X-Embodiment (O’Neill et al., 2024)) for robot action trajectories. All videos are resized and cropped to 480p, and action annotations are temporally aligned by interpolating to every 4 frames, matching the temporal compression of the video VAE. Together, these datasets provide complementary action signals (vehicle, camera, and robot pose) that support unified action-aware world modeling. For evaluation, we construct Astra-Bench, a benchmark comprising 20 held-out samples from each dataset, designed to cover a diverse range of real-world scenarios.

Training details. We initialize our model from the pre-trained video diffusion model (Wan et al., 2025) and train on $8 \times$ H800 (80G) GPUs with a per-GPU batch size of 1. Optimization is performed with AdamW (Loshchilov & Hutter, 2017) using a learning rate of $1e - 5$ for 30 epochs, requiring about 24 hours to converge. The training is conducted in the latent space of a 3D VAE. In pixel space, the number of condition frames is randomly sampled from [1, 128], while the number of target frames is fixed to 33. Additional implementation details are provided in Section A.

Metrics. Astra-Bench evaluates two key aspects of world models: visual quality and instruction following (camera motion tracking), using six fine-grained metrics. For instruction following, we assess whether generated videos accurately reflect intended walking directions and camera movements. While pose estimation tools such as MegaSaM (Li et al., 2025b) can automate this process, inaccuracies in camera motion prediction and quantization errors limit their reliability. We therefore adopt human evaluation to ensure accurate assessment. For the remaining dimensions—subject consistency, background consistency, motion smoothness, aesthetic quality, and image fidelity—we adopt metrics from VBBench (Huang et al., 2024). All test videos are generated at 480×832 resolution, 20 FPS, and 96 frames, using 50 inference steps for every model.

4.2 MAIN RESULTS

We evaluate our method on Astra-Bench and compare it against recent state-of-the-art video generation and world modeling approaches, including Wan-2.1 (Wan et al., 2025), Matrix-Game (He et al., 2025) and YUME (Mao et al., 2025). As shown in Table 1, our method consistently outperforms baselines across all metrics, demonstrating strong advantages in both visual quality and action-conditioned responsiveness. Astra achieves consistently superior results, surpassing existing video generation and world modeling approaches in both fidelity and controllability. Our model produces videos with sharper details, smoother motion, and stronger temporal coherence (Figure 5),

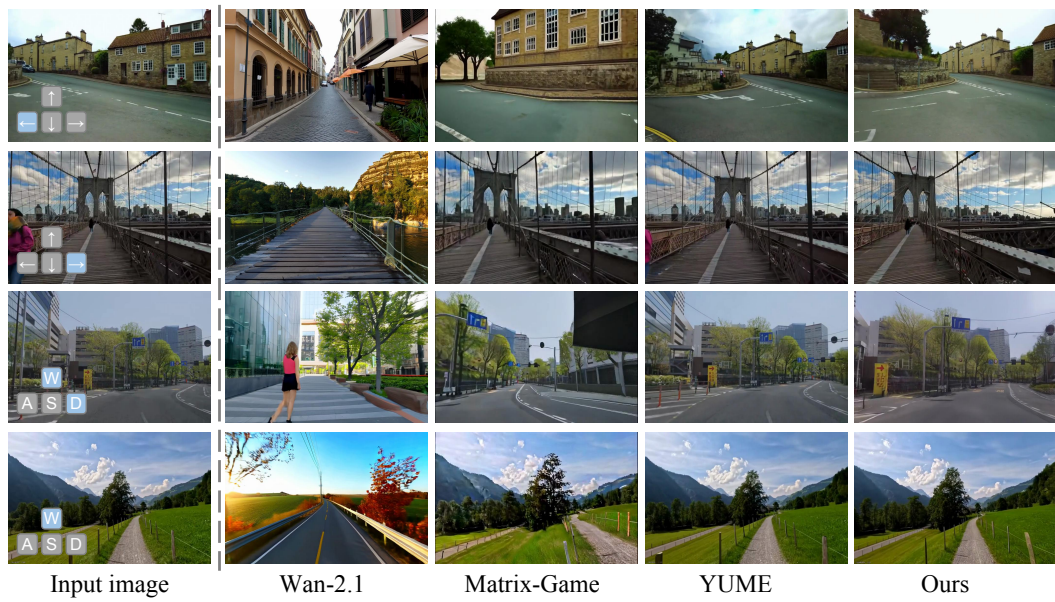


Figure 6: **Qualitative comparisons on action-driven real-world exploration.** Given the initial image and action sequence, Astra generates exploration sequences that maintain strong visual fidelity, coherent dynamics, and accurate responsiveness to user-specified actions.

Table 1: **Quantitative comparison of different models.** Astra demonstrates superior visual quality and instruction-following performance across a variety of real-world scenarios.

Method	Instruction Following \uparrow	Subject Consistency \uparrow	Background Consistency \uparrow	Motion Smoothness \uparrow	Aesthetic Quality \uparrow	Imaging Quality \uparrow
Wan-2.1 (Wan et al., 2025)	0.061	0.854	0.903	0.958	0.489	0.691
MatrixGame (He et al., 2025)	0.268	0.916	0.928	0.981	0.441	0.748
Yume (Mao et al., 2025)	0.652	0.936	0.938	0.985	0.523	0.741
Astra (Ours)	0.669	0.939	0.945	0.989	0.531	0.747

leading to higher scores on visual quality metrics such as subject and background consistency, motion smoothness, and overall aesthetic appeal. More importantly, it demonstrates a clear advantage in instruction following: human evaluations confirm that the generated trajectories more faithfully follow intended camera movements and action directions compared to prior methods. Importantly, while competing approaches often suffer from error accumulation and drift during long rollouts, Astra maintains stability across extended horizons (Figure 6), making it particularly suitable for real-world interactive scenarios where both high fidelity and reliable action following are critical.

4.3 ANALYSIS

Action integration via ACT-Adapter. Our lightweight ACT-Adapter provides an efficient way to inject action features into the pre-trained flow transformer. Freezing most parameters while tuning only the adapter and attention layers ensures maximum reuse of generative knowledge. Ablation results (Table 2, cross attn. adapter) demonstrate that ACT-Adapter achieves stronger action-conditioned performance than the cross-attention adapter used in He et al. (2025), confirming its effectiveness as a simple yet powerful extension for enhancing interactivity.

Action-free guidance enhances action responsiveness. We find that action-free guidance effectively amplifies the influence of action signals during inference. By learning to predict both with and without actions, the model gains stronger controllability, achieving sharper responses to commands while preserving stability. As shown in Table 2 (w/o AFG), this mechanism proves particularly useful for improving action responsiveness in long video rollouts.

Noisy memory mitigates visual inertia. The proposed noise-as-mask strategy alleviates the issue of visual inertia by weakening the dominance of historical context over action inputs. This encourages

432 Table 2: **Ablation studies.** We assess the contribution of each component in Astra, ensuring all
 433 experiments are conducted using the same random seed for fair comparison.

Method	Instruction Following ↑	Subject Consistency ↑	Background Consistency ↑	Motion Smoothness ↑	Aesthetic Quality ↑	Imaging Quality ↑
w/o AFG	0.545	0.841	0.892	0.957	0.492	0.703
w/o noise	0.359	0.903	0.927	0.979	0.523	0.739
cross attn. adapter	0.642	0.926	0.903	0.948	0.512	0.694
w/o MoAE	0.651	0.930	0.941	0.975	0.520	0.727
Astra (Ours)	0.669	0.939	0.945	0.989	0.531	0.747

442 the model to rely on external controls rather than simply extrapolating from past frames. As shown
 443 in Table 2 (w/o noise), the model achieves stronger responsiveness to abrupt or unexpected actions,
 444 while still maintaining long-term temporal coherence and stability in video generation.

446 **Adapting to diverse scenarios with MoAE.** MoAE allows Astra to process diverse action modalities
 447 in a unified way. By routing inputs to modality-specialized experts, it provides both versatility
 448 and precision across domains such as robotics and navigation. While joint training on heterogeneous
 449 datasets may slightly reduce performance on any single scenario, MoAE greatly improves
 450 cross-domain generalization and enables broader data usage—critical for real-world applications.
 451 Our ablation in Table 2 (w/o MoAE), trained only on camera-action data since it cannot process
 452 other modalities, further shows that MoAE markedly improves action-conditioned video generation.

453 4.4 EXTENDED APPLICATIONS

456 Our interactive world model is not limited to standard video prediction benchmarks—it naturally
 457 extends to a wide range of real-world applications. Thanks to its balanced design of action-aware
 458 conditioning, noise-augmented memory, and modular action encoding, the model can flexibly adapt
 459 to diverse tasks such as camera control, manipulation video prediction, long-horizon exploration,
 460 and autonomous driving. This versatility arises from unifying temporal consistency with responsive
 461 action integration, making it a general-purpose framework for simulating, interacting with, and
 462 editing dynamic environments. Qualitative results are provided in Section C and Figure A.

463 **Autonomous driving.** We extend Astra to autonomous driving using the nuScenes dataset (Caesar
 464 et al., 2020), which provides multi-view videos and diverse traffic contexts. Given ego-vehicle ob-
 465 servations and discrete control actions (e.g., turn left, move forward), Astra generates realistic future
 466 driving videos that capture vehicle motion, road geometry, and agent interactions. Its combination
 467 of long-term coherence and precise action responsiveness enables interactive driving simulation.

468 **Camera control.** Astra supports interactive camera control through action signals specifying cam-
 469 era trajectories such as panning and viewpoint shifts. Conditioned on these poses, it generates videos
 470 that follow instructed motions while maintaining spatial and temporal consistency. This enables con-
 471 trollable, cinematic camera movement for both creative and practical applications.

472 **Manipulation video prediction** In robotic settings, Astra predicts future video chunks conditioned
 473 on current observations and manipulation actions, simulating fine-grained interactions such as grasp-
 474 ing or tool use with high fidelity and temporal coherence. These predictive rollouts support planning,
 475 policy learning, and safe exploration in robot learning.

477 5 CONCLUSION

479 In this work, we present Astra, a simple yet effective framework for building interactive world
 480 models that unify real-world video prediction with precise action conditioning. By equipping a pre-
 481 trained video diffusion backbone with a lightweight action-aware adapter, a noise-augmented mem-
 482 ory for balancing history and responsiveness, and a mixture of action experts for versatile control,
 483 our model achieves interactive, consistent, and versatile video generation across diverse real-world
 484 scenarios. Extensive experiments show long-term consistency, visual fidelity, and instruction fol-
 485 lowing. We believe Astra offers a practical path toward more general, scalable simulators for world
 modeling in exploration, robotics, autonomous driving, and embodied intelligence.

486 REFERENCES
487

488 Niket Agarwal, Arslan Ali, Maciej Bala, Yogesh Balaji, Erik Barker, Tiffany Cai, Prithvijit Chat-
489 topadhyay, Yongxin Chen, Yin Cui, Yifan Ding, et al. Cosmos world foundation model platform
490 for physical ai. *arXiv preprint arXiv:2501.03575*, 2025.

491 Jianhong Bai, Menghan Xia, Xiao Fu, Xintao Wang, Lianrui Mu, Jinwen Cao, Zuozhu Liu, Haoji
492 Hu, Xiang Bai, Pengfei Wan, et al. Recammaster: Camera-controlled generative rendering from
493 a single video. *arXiv preprint arXiv:2503.11647*, 2025.

494 Amir Bar, Gaoyue Zhou, Danny Tran, Trevor Darrell, and Yann LeCun. Navigation world models.
495 In *CVPR*, pp. 15791–15801, 2025.

496 Andreas Blattmann, Tim Dockhorn, Sumith Kulal, Daniel Mendelevitch, Maciej Kilian, Dominik
497 Lorenz, Yam Levi, Zion English, Vikram Voleti, Adam Letts, et al. Stable video diffusion: Scaling
498 latent video diffusion models to large datasets. *arXiv preprint arXiv:2311.15127*, 2023.

499 500 Anthony Brohan, Noah Brown, Justice Carbajal, Yevgen Chebotar, Joseph Dabis, Chelsea Finn,
501 Keerthana Gopalakrishnan, Karol Hausman, Alex Herzog, Jasmine Hsu, et al. Rt-1: Robotics
502 transformer for real-world control at scale. *arXiv preprint arXiv:2212.06817*, 2022.

503 504 Tim Brooks, Bill Peebles, Connor Holmes, Will DePue, Yufei Guo, Li Jing, David Schnurr, Joe
505 Taylor, Troy Luhman, Eric Luhman, et al. Video generation models as world simulators. *URL*
506 <https://openai.com/research/video-generation-models-as-world-simulators>, 3, 2024.

507 508 Jake Bruce, Michael D Dennis, Ashley Edwards, Jack Parker-Holder, Yuge Shi, Edward Hughes,
509 Matthew Lai, Aditi Mavalankar, Richie Steigerwald, Chris Apps, et al. Genie: Generative inter-
510 active environments. In *ICML*, 2024.

511 512 Holger Caesar, Varun Bankiti, Alex H Lang, Sourabh Vora, Venice Erin Liong, Qiang Xu, Anush
513 Krishnan, Yu Pan, Giancarlo Baldan, and Oscar Beijbom. nuscenes: A multimodal dataset for
514 autonomous driving. In *CVPR*, pp. 11621–11631, 2020.

515 516 Jun Cen, Chaohui Yu, Hangjie Yuan, Yuming Jiang, Siteng Huang, Jiayan Guo, Xin Li, Yibing
517 Song, Hao Luo, Fan Wang, et al. Worldvla: Towards autoregressive action world model. *arXiv
preprint arXiv:2506.21539*, 2025.

518 519 Prafulla Dhariwal and Alexander Nichol. Diffusion models beat gans on image synthesis. *NeurIPS*,
520 34:8780–8794, 2021.

521 522 Hao He, Yinghao Xu, Yuwei Guo, Gordon Wetzstein, Bo Dai, Hongsheng Li, and Ceyuan Yang.
Cameractrl: Enabling camera control for text-to-video generation. *CoRR*, 2024.

523 524 Xianglong He, Chunli Peng, Zexiang Liu, Boyang Wang, Yifan Zhang, Qi Cui, Fei Kang, Biao
525 Jiang, Mengyin An, Yangyang Ren, et al. Matrix-game 2.0: An open-source, real-time, and
526 streaming interactive world model. *arXiv preprint arXiv:2508.13009*, 2025.

527 528 Roberto Henschel, Levon Khachatryan, Hayk Poghosyan, Daniil Hayrapetyan, Vahram Tadevosyan,
529 Zhangyang Wang, Shant Navasardyan, and Humphrey Shi. Streamingt2v: Consistent, dynamic,
and extendable long video generation from text. In *CVPR*, pp. 2568–2577, 2025.

530 531 Jonathan Ho, Ajay Jain, and Pieter Abbeel. Denoising diffusion probabilistic models. *NeurIPS*, 33:
532 6840–6851, 2020.

533 534 Jonathan Ho, Tim Salimans, Alexey Gritsenko, William Chan, Mohammad Norouzi, and David J
Fleet. Video diffusion models. *NeurIPS*, 35:8633–8646, 2022.

535 536 Siqiao Huang, Jialong Wu, Qixing Zhou, Shangchen Miao, and Mingsheng Long. Vid2world: Craft-
537 ing video diffusion models to interactive world models. *arXiv preprint arXiv:2505.14357*, 2025.

538 539 Ziqi Huang, Yinan He, Jiashuo Yu, Fan Zhang, Chenyang Si, Yuming Jiang, Yuanhan Zhang, Tianx-
ing Wu, Qingyang Jin, Nattapol Chanpaisit, et al. Vbench: Comprehensive benchmark suite for
video generative models. In *CVPR*, pp. 21807–21818, 2024.

540 Zhen Li, Chuanhao Li, Xiaofeng Mao, Shaoheng Lin, Ming Li, Shitian Zhao, Zhaopan Xu, Xinyue
 541 Li, Yukang Feng, Jianwen Sun, et al. Sekai: A video dataset towards world exploration. *arXiv*
 542 *preprint arXiv:2506.15675*, 2025a.

543

544 Zhengqi Li, Richard Tucker, Forrester Cole, Qianqian Wang, Linyi Jin, Vickie Ye, Angjoo
 545 Kanazawa, Aleksander Holynski, and Noah Snavely. Megasam: Accurate, fast and robust struc-
 546 ture and motion from casual dynamic videos. In *CVPR*, pp. 10486–10496, 2025b.

547 Hao Liu, Wilson Yan, Matei Zaharia, and Pieter Abbeel. World model on million-length video and
 548 language with blockwise ringattention. *arXiv preprint arXiv:2402.08268*, 2024.

549

550 Xinhao Liu, Jintong Li, Yicheng Jiang, Niranjan Sujay, Zhicheng Yang, Juexiao Zhang, John
 551 Abanes, Jing Zhang, and Chen Feng. Citywalker: Learning embodied urban navigation from
 552 web-scale videos. In *CVPR*, pp. 6875–6885, 2025.

553 Ilya Loshchilov and Frank Hutter. Decoupled weight decay regularization. *arXiv preprint*
 554 *arXiv:1711.05101*, 2017.

555

556 Xin Ma, Yaohui Wang, Gengyun Jia, Xinyuan Chen, Ziwei Liu, Yuan-Fang Li, Cunjian Chen,
 557 and Yu Qiao. Latte: Latent diffusion transformer for video generation. *arXiv preprint*
 558 *arXiv:2401.03048*, 2024.

559

560 Xiaofeng Mao, Shaoheng Lin, Zhen Li, Chuanhao Li, Wenshuo Peng, Tong He, Jiangmiao Pang,
 561 Mingmin Chi, Yu Qiao, and Kaipeng Zhang. Yume: An interactive world generation model. *arXiv*
 562 *preprint arXiv:2507.17744*, 2025.

563

564 Abby O'Neill, Abdul Rehman, Abhiram Maddukuri, Abhishek Gupta, Abhishek Padalkar, Abraham
 565 Lee, Acorn Pooley, Agrim Gupta, Ajay Mandlekar, Ajinkya Jain, et al. Open x-embodiment:
 566 Robotic learning datasets and rt-x models: Open x-embodiment collaboration 0. In *ICRA*, pp.
 567 6892–6903. IEEE, 2024.

568

569 William Peebles and Saining Xie. Scalable diffusion models with transformers. In *ICCV*, pp. 4195–
 570 4205, 2023.

571

572 Robin Rombach, Andreas Blattmann, Dominik Lorenz, Patrick Esser, and Björn Ommer. High-
 573 resolution image synthesis with latent diffusion models. In *CVPR*, pp. 10684–10695, 2022.

574

575 Olaf Ronneberger, Philipp Fischer, and Thomas Brox. U-net: Convolutional networks for biomedical
 576 image segmentation. In *MICCAI*, pp. 234–241. Springer, 2015.

577

578 Jiaming Song, Chenlin Meng, and Stefano Ermon. Denoising diffusion implicit models. In *ICLR*,
 579 2020.

580

581 Kiwhan Song, Boyuan Chen, Max Simchowitz, Yilun Du, Russ Tedrake, and Vincent Sitzmann.
 582 History-guided video diffusion. *arXiv preprint arXiv:2502.06764*, 2025.

583

584 Hansi Teng, Hongyu Jia, Lei Sun, Lingzhi Li, Maolin Li, Mingqiu Tang, Shuai Han, Tianning
 585 Zhang, WQ Zhang, Weifeng Luo, et al. Magi-1: Autoregressive video generation at scale. *arXiv*
preprint arXiv:2505.13211, 2025.

586

587 Team Wan, Ang Wang, Baole Ai, Bin Wen, Chaojie Mao, Chen-Wei Xie, Di Chen, Feiwu Yu,
 588 Haiming Zhao, Jianxiao Yang, et al. Wan: Open and advanced large-scale video generative
 589 models. *arXiv preprint arXiv:2503.20314*, 2025.

590

591 Jiahao Wang, Yufeng Yuan, Ruijie Zheng, Youtian Lin, Jian Gao, Lin-Zhuo Chen, Yajie Bao,
 592 Yi Zhang, Chang Zeng, Yanxi Zhou, et al. Spatialvid: A large-scale video dataset with spatial
 593 annotations. *arXiv preprint arXiv:2509.09676*, 2025.

594

595 Xiaofeng Wang, Zheng Zhu, Guan Huang, Boyuan Wang, Xinze Chen, and Jiwen Lu. World-
 596 dreamer: Towards general world models for video generation via predicting masked tokens. *arXiv*
 597 *preprint arXiv:2401.09985*, 2024.

598

599 Jialong Wu, Shaofeng Yin, Ningya Feng, Xu He, Dong Li, Jianye Hao, and Mingsheng Long.
 600 ivideogpt: Interactive videogogs are scalable world models. *NeurIPS*, 37:68082–68119, 2024.

594 Zhuoyi Yang, Jiayan Teng, Wendi Zheng, Ming Ding, Shiyu Huang, Jiazheng Xu, Yuanming Yang,
595 Wenyi Hong, Xiaohan Zhang, Guanyu Feng, et al. Cogvideox: Text-to-video diffusion models
596 with an expert transformer. 2025.

597 Lvmi Zhang and Maneesh Agrawala. Packing input frame context in next-frame prediction models
598 for video generation, 2025. URL <https://arxiv.org/abs/2504.12626>.

600 Zangwei Zheng, Xiangyu Peng, Tianji Yang, Chenhui Shen, Shenggui Li, Hongxin Liu, Yukun
601 Zhou, Tianyi Li, and Yang You. Open-sora: Democratizing efficient video production for all.
602 URL <https://github.com/hpcaltech/Open-Sora>, 2024.

603
604
605
606
607
608
609
610
611
612
613
614
615
616
617
618
619
620
621
622
623
624
625
626
627
628
629
630
631
632
633
634
635
636
637
638
639
640
641
642
643
644
645
646
647

648
649
650
651 Table A: Datasets used in experiments, along with their actions and sample sizes. For each dataset,
652 we list the action type, followed by the dimensionality of its representation.

651 Dataset	652 Action	653 Scenario	654 Size
652 nuScenes (Caesar et al., 2020)	653 Camera (7)	654 Autonomous driving	655 850
653 Sekai (Li et al., 2025a)	654 Camera (12)	655 Walking & drone view	656 50K
654 SpatialVid (Wang et al., 2025)	655 Camera (7) & keyboard / mouse	656 In-the-wild videos	657 200K
655 RT-1 (Brohan et al., 2022)	656 Robotic pose (7)	657 Robot manipulation	658 9978
656 Multi-Cam Video (Bai et al., 2025)	657 Camera (12)	658 Human motion	659 136K
660 Total			661 $\sim 397K$ (360 hours)

662 A MORE EXPERIMENTAL DETAILS

663 A.1 DATASETS

664 We use the training data sampled from the nuScenes (Caesar et al., 2020), Sekai (Li et al., 2025a),
665 SpatialVID (Wang et al., 2025), Multi-Cam Video (Bai et al., 2025) and RT-1 (Brohan et al., 2022).
666 To ensure balanced exposure across these datasets, we apply a set of sampling weights that control
667 the frequency with which data from each source is drawn during training. A summary of dataset
668 statistics is provided in Table A, with detailed descriptions reported as follows:

669 **nuScenes:** nuScenes is an autonomous vehicle dataset collected from an AV approved for testing on
670 public roads and it contains the full 360° sensor suite (lidar, images, and radar). It comprises 1000
671 scenes, each 20s long and fully annotated with 3D bounding boxes for 23 classes and 8 attributes.
672 We use its 7 dimensions pose parts as our action.

673 **Sekai:** Sekai is a high-quality first-person view worldwide video dataset with rich annotations for
674 world exploration. It consists of over 5,000 hours of walking or drone view (FPV and UVA) videos
675 from over 100 countries and regions across 750 cities. The action of this dataset is the camera pose.

676 **SpatialVID:** SpatialVID is a dataset consisting of a large corpus of in-the-wild videos with diverse
677 scenes, camera movements and dense 3D annotations such as per-frame camera poses, depth, and
678 motion instructions. SpatialVID has a total of 7,089 hours of dynamic content. We use the 7-
679 dimensional camera parts as our action.

680 **RT-1:** RT-1 is a large, diverse dataset of robot trajectories that includes multiple tasks, objects and
681 environments. It contains over 130k individual demonstrations constituting over 700 distinct task
682 instructions using a large variety of objects. We use its 7 dimensions ee-space pose parts as our
683 action. We use Open X-Embodiment (O’Neill et al., 2024) version of the RT-1 dataset.

684 **Multi-Cam Video:** Multi-Cam Video is a synthetic dataset rendered with multiple cameras cap-
685 turing the same scene simultaneously. Animated characters are placed in diverse 3D environments,
686 while cameras follow predefined trajectories to simulate synchronized shooting. We use 10K videos
687 with detailed camera annotations as action signals.

688 A.2 TRAINING DETAILS

689 We initialize our model using the pre-trained weights of the Wan-2.1 base model (Wan et al., 2025).
690 Our training is run on 8 H800 (80G) with a per-GPU batch size of 1. We train our model with
691 AdamW (Loshchilov & Hutter, 2017) optimizer and a learning rate of $1e-5$ for 30 epochs. Our
692 training runs take approximately 24 hours to converge. All videos are resized and cropped to the
693 training resolution (480×832). The model is trained on the latent space produced by a 3D VAE. In
694 pixel space, the count of condition frames is randomly sampled from the range [1, 128], whereas the
695 number of target frames is consistently set to 33.

696 A.3 MODEL ARCHITECTURE

697 Our framework builds on Wan-2.1 (Wan et al., 2025), a large-scale video diffusion model composed
698 of 30 stacked flow transformer (DiT-style) blocks, each containing multi-head self-attention and
699 feed-forward layers with residual connections. Wan-2.1 serves as a strong pre-trained backbone,
700 providing rich generative priors for high-quality video synthesis. To enable interactive control, we

Table B: Quantitative action-alignment comparison. We complement the human-rated instruction-following metric by reporting rotation and translation errors that directly measure how well generated camera motions align with the commanded actions.

Method	RotErr \downarrow	TransErr \downarrow	Instruction Following \uparrow	Imaging Quality \uparrow
Wan-2.1 (Wan et al., 2025)	2.96	7.37	0.061	0.691
YUME (Mao et al., 2025)	2.20	5.80	0.268	0.741
MatrixGame (He et al., 2025)	2.25	5.63	0.652	0.748
NWM (Bar et al., 2025)	2.47	6.13	0.311	0.635
Astra (ours)	1.23	4.86	0.669	0.747

introduce two lightweight yet effective extensions: ACT-Adapter and Mixture of Action Experts (MoAE). The ACT-Adapter is implemented as a single linear layer inserted after each self-attention block. It is initialized as an identity mapping and fine-tuned jointly with the attention parameters, allowing the model to inject action features into the latent space while preserving stability of the pre-trained weights. In parallel, MoAE provides a modular action encoding mechanism. It consists of a linear router that projects heterogeneous action modalities into a shared space, followed by a set of MLP-based experts specialized for different action types. Specifically, we support camera control actions represented as 7 or 12-dimensional vectors, robotic actions represented as 7-dimensional vectors, and navigation commands expressed through discrete keyboard and mouse inputs. The routed outputs are combined into a unified representation that is fed into the ACT-Adapter, ensuring both precision and versatility. Together, these components augment Wan-2.1 into an autoregressive denoising model capable of faithfully following actions while maintaining long-horizon temporal coherence. During inference, we set the scale s for action-free guidance (AFG) to be 3.0.

A.4 METRIC DETAILS.

We follow YUME (Mao et al., 2025) to use human evaluation and VBench (Huang et al., 2024) metrics to assess the performance of our model. For instruction following, automated camera-motion estimators (e.g., MegaSaM (Li et al., 2025b)) can provide approximate motion labels, but their predictions often suffer from inaccuracies and quantization errors, especially under complex scene geometry or fast motion. To ensure reliable assessment, we therefore rely purely on human evaluation. Specifically, we recruit 20 users to inspect each generated sequence together with the corresponding action command. The instruction-following score is computed as the ratio of users who agree that the generated motion faithfully reflects the specified action direction and action type. For a more objective evaluation, we follow prior works (Bai et al., 2025; He et al., 2024) and measure how closely the camera motion in the generated video matches the ground-truth trajectory, using MegaSaM to estimate camera poses. As shown in Table B, Astra achieves lower rotation and translation errors than existing methods, consistent with the human-rated instruction-following results. Together, these metrics offer a fine-grained quantitative view of action alignment, further demonstrating the precise interactive control enabled by our model.

A.5 PARAMETER ANALYSIS.

Astra is designed to be lightweight, adding far fewer parameters than prior interactive world models such as YUME (Mao et al., 2025) and MatrixGame (He et al., 2025). As shown in Table C, MatrixGame introduces heavy cross-attention modules and large action encoders, resulting in significant training and inference overhead, while YUME depends on a much larger 13B backbone. In contrast, Astra adds only two small components: ACT-Adapter (a single linear layer after each self-attention block) and MoAE (a lightweight linear router plus small MLP experts, with only one expert active per step).

These additions contribute only a minor increase in parameters, making Astra the most parameter-efficient model among the compared methods. Because the backbone remains frozen and the added modules are shallow, the computation cost is nearly unchanged, enabling fast, stable training

756 **Table C: Parameter comparison.** Astra introduces the smallest parameter overhead among all
 757 methods, adding only lightweight adapters while preserving the efficiency of the frozen backbone.
 758

Method	Base model	Trainable Params.	Note
NVM (Bar et al., 2025)	CDiT-XL	~ 1B	Full tuning
YUME (Mao et al., 2025)	Wan2.1-14B	~ 14B	Full tuning
MatrixGame (He et al., 2025)	Wan2.1-1.3B	~ 1.8B	Full tuning, cross-attn adapters
Astra (ours)	Wan2.1-1.3B	366.8M	Tuning adapters & self-attn.

765 Table D: Comparative overview of various world model methods, detailing their respective domains
 766 of application, supported control modalities, and interaction horizons.
 767

Method	Domain	Control	Interaction Horizon
Wan-2.1 (Wan et al., 2025)	General	Text	A few seconds
MatrixGame (He et al., 2025)	Game-specific	Keyboard / Mouse	A few seconds
YUME (Mao et al., 2025)	Walking-specific	Keyboard / Mouse	8-10 seconds
Astra (Ours)	General	Camera; Keyboard / Mouse; Robot pose	8-10 seconds

766 and long-horizon rollout without heavy architectural modifications. Overall, Astra achieves strong
 767 action-conditioned performance with the lowest parameter and compute overhead in its class.
 768

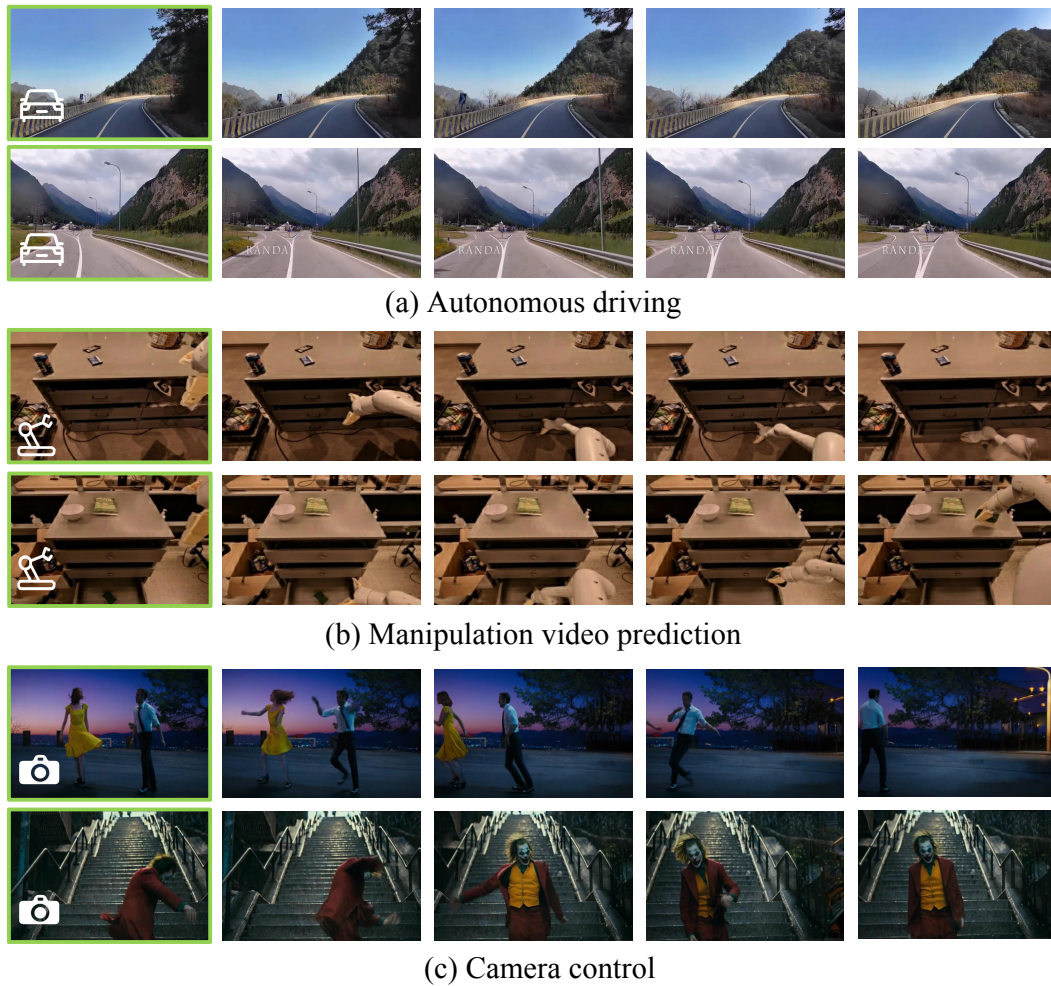
780 B COMPARISON WITH EXISTING WORLD MODELS

782 Table D compares four representative world models—Wan-2.1 (Wan et al., 2025), MatrixGame (He
 783 et al., 2025), YUME (Mao et al., 2025), and Astra—across three key dimensions: domain, control
 784 modality, and interaction horizon. In terms of domain, Astra is designed for general-purpose scenarios,
 785 showcasing their versatility in a wide range of applications. MatrixGame, however, is tailored
 786 specifically for game-related contexts, limiting its use to game-specific environments. YUME fo-
 787 cuses on walking-specific domains, which is a niche area compared to the general-purpose methods.
 788 For control modalities, Wan-2.1 relies solely on text input, reflecting a language-driven paradigm.
 789 MatrixGame and YUME adopt traditional keyboard and mouse controls. Astra, enabled by MoAE,
 790 supports multiple modalities—including camera input, keyboard/mouse, and robot pose—providing
 791 more flexible and intuitive interaction. Finally, regarding the interaction horizon, Wan-2.1 and Ma-
 792 trixGame are limited to short spans of a few seconds. YUME extends this to 8–10 seconds, and As-
 793 tra matches this longer horizon through noisy memory and the input-packing technique of (Zhang
 794 & Agrawala, 2025). Combined with its multi-modal control and general-purpose domain, Astra
 795 emerges as the most comprehensive solution among the compared methods.

796 C MORE RESULTS

798 C.1 EXTENDED APPLICATIONS.

800 As shown in Figure A, our Astra framework is designed to generalize across a wide range of in-
 801 teractive video prediction tasks, demonstrating strong adaptability in domains such as autonomous
 802 driving, robotic manipulation, and camera control. In driving scenarios, Astra generates realistic
 803 long-horizon rollouts that capture complex road dynamics while responding accurately to control
 804 signals like steering or acceleration. For manipulation, it predicts object interactions conditioned on
 805 robot actions, enabling fine-grained and physically consistent outcomes. In camera control, Astra
 806 follows viewpoint instructions such as panning, zooming, or rotation, while maintaining temporal
 807 and visual coherence. Together, these applications highlight Astra’s versatility and effectiveness as
 808 a unified world modeling framework capable of handling heterogeneous action modalities in diverse
 809 real-world settings.



842 **Figure A: Extended applications of Astra.** Our framework handles diverse scenarios: (a) au-
843 tonomous driving, predicting long-horizon traffic dynamics from control inputs; (b) manipu-
844 lation, conditioning robot actions on object interactions; and (c) camera control, reflecting viewpoint
845 changes in coherent videos. These demonstrate Astra’s versatility for interactive world modeling.

846 C.2 OUT-OF-DOMAIN GENERALIZATION.

848 We further evaluate Astra on out-of-domain (OOD) scenes—including indoor environments, styl-
849 ized anime videos, and even Minecraft gameplay—none of which are present in the training distri-
850 bution. Across all cases in [Figure B](#), Astra produces coherent, action-conditioned rollouts: given
851 camera or navigation commands, it generates futures that accurately follow the instructed motion
852 while maintaining global structure and temporal consistency. In indoor scenes, the model handles
853 complex layouts and viewpoint shifts; in anime clips, it remains responsive despite fast and unpre-
854 dictable dynamics; and in Minecraft, it adapts to drastically different textures and rendering styles
855 while still executing the intended camera movement. These results show that Astra’s autoregressive
856 denoising framework, noise-augmented memory, and action-aware conditioning generalize effec-
857 tively under substantial distribution shift. We also present two examples applying different complex
858 action sequences to the same scene (Rows 3 and 4 in [Figure B](#)), both of which are followed faithfully.

859 860 C.3 MULTI-AGENT INTERACTION.

861 In [Figure C](#), we illustrate Astra’s ability to handle multi-agent scenarios through a first-person driv-
862 ing example where the ego-vehicle overtakes two cars. Conditioned on a sequence of action com-

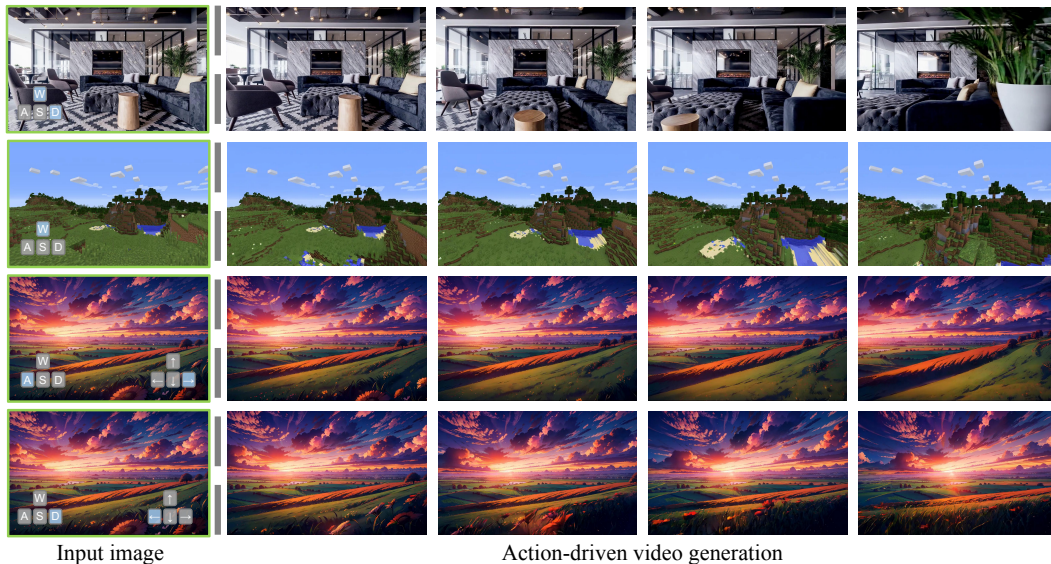


Figure B: **Out-of-domain generation results of Astra.** Astra generalizes to scenes not seen during training, including indoor environments, Minecraft worlds, and animation-style scenes, producing coherent futures that follow camera or navigation commands. The last two rows show two distinct complex action sequences executed within the same scene.



Figure C: **Multi-agent interaction of Astra.** Given a specified action sequence, Astra generates smooth, realistic multi-agent interactions, such as an ego-vehicle overtaking other cars.

mands, the model produces a coherent rollout that follows the specified trajectory while plausibly simulating the motions of surrounding vehicles. This highlights that Astra’s autoregressive denoising process, noise-augmented memory, and MoAE-based action conditioning together enable stable multi-agent interactions with accurate action following.

C.4 COMPARISONS WITH MORE METHODS.

To more comprehensively situate Astra within the broader landscape of visual world modeling, we provide extended quantitative and qualitative comparisons with additional state-of-the-art approaches. Specifically, we compare against methods such as Navigation World Models (NVM) (Bar et al., 2025) in Figure D and Table B, which are representative of recent approaches integrating multimodal inputs and action-conditioned predictions. Our results demonstrate that Astra achieves competitive or superior performance across key metrics, including visual fidelity, temporal consistency, and action responsiveness. While direct numerical comparisons are limited by differences in evaluation protocols and datasets, qualitative visualizations show that Astra generates long-horizon, coherent videos that faithfully follow user-specified actions, outperforming prior methods in capturing the causal dynamics of the environment. These comparisons highlight Astra’s ability to combine accurate action conditioning with long-term rollout stability, confirming its effectiveness as a general interactive world model across diverse scenarios. It is worth noting that many of the most advanced world models, such as Genie-3 (Bruce et al., 2024), are currently closed-source or provide only limited evaluation interfaces, making direct numerical comparison infeasible.



918
919
920
921
922
923
924
925
926
927
928
929
930
931
932
933
934
935
936
937
938
939
940
941
942
943
944
945
946
947
948
949
950
951
952
953
954
955
956
957
958
959
960
961
962
963
964
965
966
967
968
969
970
971
Figure D: **Qualitative comparison with NVM** (Bar et al., 2025). Astra consistently produces visually coherent results while faithfully following action inputs.

Table E: **Quantitative comparison on CityWalker dataset.** Astra consistently achieves higher visual quality and more reliable action following when evaluated on fully unseen scenes.

Method	Instruction Following \uparrow	Subject Consistency \uparrow	Background Consistency \uparrow	Motion Smoothness \uparrow	Aesthetic Quality \uparrow	Imaging Quality \uparrow
Wan-2.1 (Wan et al., 2025)	0.084	0.827	0.843	0.913	0.417	0.632
MatrixGame (He et al., 2025)	0.247	0.923	0.939	0.946	0.426	0.653
Yume (Mao et al., 2025)	0.619	0.933	0.927	0.972	0.511	0.628
Astra (Ours)	0.641	0.948	0.944	0.983	0.554	0.695

C.5 QUANTITATIVE COMPARISONS ON LARGER DATASETS.

To further address concerns about evaluation scale, we conduct an expanded study on a larger held-out set from the CityWalker (Liu et al., 2025) dataset. CityWalker is an egocentric urban navigation corpus collected from in-the-wild YouTube walking videos with pose estimates. We sample 100 scene images, each paired with its future ground-truth action trajectory, producing 100 long-horizon rollouts that robustly test cross-scene generalization and action adherence. Across this larger evaluation, Astra consistently achieves the best action-following accuracy and video quality, outperforming all baselines in metrics such as motion consistency, temporal stability, and VBench perceptual scores (Table E). These results confirm that Astra’s strong performance is not an artifact of small-set evaluation, and that the model maintains robust generalization and reliable action responsiveness even under substantially expanded test conditions.

D DISCUSSION ON VISUAL INERTIA.

Previous work (Zhang & Agrawala, 2025) has shown that longer video context can improve generation quality. However, in interactive world modeling, we observe that increasing context length can reduce action responsiveness. We term this phenomenon *visual inertia*—the model’s tendency to over-rely on past visual frames while neglecting user actions. To examine this, we train Astra with different history lengths without our proposed noisy-memory mechanism. As shown in Figure E, the action-following score drops substantially as context length increases, indicating that overly clean and long visual histories can dominate the model’s decision process. This motivates our noise-augmented memory design, which intentionally reduces visual dominance and encourages the model to integrate both historical context and action signals when generating future frames.

E LIMITATIONS

Despite the promising performance of Astra, our framework still faces limitations in inference efficiency. Since it builds on diffusion-based generation with autoregressive rollouts, producing long-

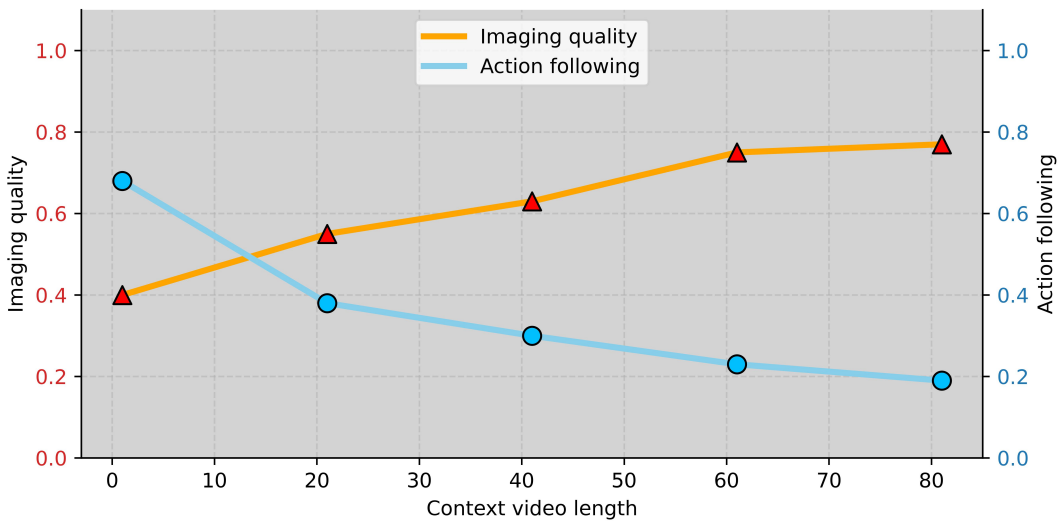


Figure E: **Effect of visual inertia.** As the history length increases, video quality improves, but the action-following score drops sharply, illustrating the visual inertia phenomenon.

horizon interactive videos requires multiple denoising steps per frame, making real-time deployment challenging. This constraint limits its applicability in latency-sensitive scenarios such as online control or interactive robotics. To address this, future work could explore distillation or student-teacher compression strategies that retain the fidelity and responsiveness of Astra while reducing inference cost, thereby paving the way for lightweight, real-time world modeling.

F CODES & DEMOS

The complete source code and demo videos for our method is provided in the `./code` and `./videos` folder, which contains the required files to reproduce our experiments with the Astra framework.

1003
1004
1005
1006
1007
1008
1009
1010
1011
1012
1013
1014
1015
1016
1017
1018
1019
1020
1021
1022
1023
1024
1025